JOURNAL OF GUIDANCE, CONTROL, AND DYNAMICS
Vol. 21, No. 5, September–October 1998

Hysteresis and Vibration Compensation for Piezoactuators

Donald Croft* and Santosh Devasia†
University of Utah, Salt Lake City, Utah 84112-9208

Structural vibrations and hysteresis nonlinearities in piezoactuators have been fundamental limitations when using these actuators for high-speed precision-positioning applications. Positioning speed (bandwidth) is limited by structural vibrations, typically, to about one-tenth the fundamental vibrational frequency of the piezoprobe. Further, precision in positioning is limited by hysteresis nonlinearities, which can result in significant errors for large-range positioning applications. This paper shows that significant improvements in precision and bandwidth can be achieved by using an inversion-based approach to compensate for hysteresis and vibrations in the piezodynamics. The approach decouples the inversion into 1) inversion of the hysteresis nonlinearity and 2) inversion of the structural dynamics, to find an input voltage profile that achieves precision tracking of a desired position trajectory. The approach is applied to a piezoactuator, and experimental results show that an order of magnitude improvement in positioning speed is achieved, while maintaining precision tracking of the desired position trajectory.

I. Introduction

PIEZOACTUATORS can achieve nanometer resolution positioning and are hence increasingly being used for ultraprecision positioning in aerospace applications,[1,2] vibration control, scanning probe microscopy for surface characterization, and nanofabrication.[3–5] Two major limitations of present positioning techniques using piezoactuators are 1) low operating bandwidth due to positioning errors caused by structural vibrations at high speeds and 2) low precision for relatively large-range displacements (due to errors caused by hysteresis nonlinearities), resulting in restricted positioning range. This paper presents a method to improve both the accuracy and the speed of piezoactuators by using an inversion-based approach to find the voltage input to the piezoactuators that compensates for the hysteresis nonlinearities and the structural vibrations. This approach first decouples the system dynamics into two separate subsystems that model 1) the hysteresis nonlinearity and 2) the structural vibrations. These subsystems are then inverted individually. The general theory of inverse-dynamics-based control can be found in Refs. 6 and 7 for nonlinear systems. These results have also been extended to systems with nonminimum phase dynamics.[8,9] Of particular interest are works related to inversion of linear dynamics in Ref. 10, which was applied to piezoactuators in Ref. 11, where only the structural dynamics of the piezoactuator was considered. In the present paper, the results in Ref. 11 are extended to include both hysteresis and vibration effects.

A. Current Limitation: Low Positioning Speed

The bandwidth of piezoactuators is limited by the actuator system's lowest resonant vibrational frequency because structural vibrations become substantial at frequencies close to the resonant frequency and cause significant positioning errors.[12] In practice, when ultraprecision positioning is desired, these vibration-caused errors in positioning typically restrict bandwidth to significantly low frequencies (less than one-tenth of the vibrational frequency of the piezoactuator).[12–14] Faster positioning can be achieved by increasing the lowest resonant frequencies of the system, for example, by using shorter piezotubes or piezo–plate scanners[15] as actuators. However, these tend to have limited positioning ranges—if large displacements are required, then a large piezoactuator is needed (which tends to have a relatively low resonant frequency). An alternative approach is to improve the dynamic response with feedback control. However, there are limits to the improvements achievable through feedback schemes because high feedback gains tend to destabilize the system.[16,17] Even with improved feedback control, turnaround transients that occur when the direction of motion changes still substantially limit the bandwidth improvements.[16,18] These transients are proportional to the velocity changes in turnarounds, and thus any attempt to increase scan velocities increases the transient errors and thus decreases the accuracy of the tracking. In summary, the structural vibrations of the piezodynamics need to be accounted for to achieve fast positioning.

B. Current Limitation: Low Precision

In addition to the problem of low positioning speeds, another significant difficulty arises due to the hysteresis nonlinearities in the piezodynamics. Over relatively large-range displacements, hysteresis nonlinearities in the piezodynamics become significant and, if ignored, lead to significant errors in output tracking. This hysteresis effect needs to be accounted for to maintain precision positioning over relatively large ranges. Present approaches to overcome this hysteresis-caused loss of precision can be grouped into three general categories. One set of approaches consists of controlling the electric charge applied to the piezoactuator rather than controlling the voltage applied to the piezoactuator.[19–20] These approaches do alleviate some of the problems caused by nonlinearities and reduce some of the rate-dependent hysteresis phenomena. Thus, these approaches improve linearity (with some penalty on sensitivity), but they are still not sufficient for high-precision positioning. A second set of methods consists of using closed-loop control schemes to correct for the hysteresis nonlinearities. The improvements are limited by instabilities at high-feedback gains and, furthermore, aren't sufficient, especially when tracking at relatively high frequencies.[18] The third category of methods consists of modeling the hysteresis and modifying the applied voltage to compensate for the hysteresis effects; several approaches are available to model the hysteresis, for example, polynomial curves,[13,21] Preisach models,[14,22] and trigonometric functions.[23] In this paper, we integrate this third approach (to model and to compensate for hysteresis nonlinearities) with the inversion-based approach, presented in Refs. 10, 11, and 24, that accounts for structural vibrations, to achieve precision positioning even at substantially high speeds.

C. Inversion-Based Approach

Recent results have clearly demonstrated that significant improvements in bandwidth can be achieved by inverting the system dynamics to find input voltages that compensate for structural vibrations.[11] However, these results, based on inversion of linear systems,[10,11] are limited to small range position control. Over relatively large-range displacements of a piezoactuator, hysteresis nonlinearities become significant and need to be accounted for to maintain precision positioning. The approach, presented here, decouples the inversion of the piezodynamics into 1) inversion of the hysteresis nonlinearity and

Received July 14, 1997; revision received April 3, 1998; accepted for publication April 13, 1998.

*Graduate Researcher, Department of Mechanical Engineering, MEB 1202. E-mail: croft@eng.utah.edu.

†Assistant Professor, Department of Mechanical Engineering, MEB 3201. E-mail: santosh@eng.utah.edu. Member AIAA.

2) inversion of the structural dynamics, to obtain the feed-forward input voltage that achieves precision tracking of a desired output trajectory. The hysteresis is modeled as an input nonlinearity[13,14,21,22] and then inverted to linearize the system dynamics. Next, the linearized system dynamics are inverted[10,11] to obtain precision output tracking. The inversion-based approach gives exact output tracking (modulo modeling errors); in contrast, feedback-based techniques[18] may not guarantee exact tracking even with perfect knowledge of the system. Experimental verification is also presented, which shows that substantial performance improvements are possible. Positioning bandwidth was increased from one tenth of the fundamental vibrational frequency of the piezosystem to the fundamental vibrational frequency of the piezosystem (while maintaining precision output tracking).

We present the modeling of an experimental piezoactuator system in Sec. II and present the inversion technique in Sec. III. Experimental results and discussion are in Sec. IV, followed by our conclusions in Sec. V.

II. Modeling of the Piezoactuator

The key to an inversion-based approach for trajectory tracking is the development of a model that accounts for the hysteresis nonlinearities and the dynamics of the piezoactuator. The hysteresis is modeled as an input nonlinearity, and the structural vibration is modeled as a linear system; these two submodels are cascaded to obtain the complete piezoactuator model. These submodels are then inverted individually to find inputs that achieve tracking of a desired output trajectory (see Fig. 1). A similar decoupling approach has been followed in Ref. 25; however, the goal is only to model the system dynamics to predict the system-response output to an input. In contrast, we solve the inverse-dynamics problem.

Note in Fig. 1 that the voltage applied to the piezoactuator system $V_a(t)$ is first modified by the hysteresis model h. The output $u(t)$ of the hysteresis model h is a nonlinear function of the applied voltage $V_a(t)$ and also its previous time history.[14] This modified signal $u(t)$ is then applied to the linear system $G(s)$, which is represented in state-space form as

$$\dot{x}(t) = Ax(t) + Bu(t) \tag{1}$$

$$y(t) = Cx(t) \tag{2}$$

where the time derivative is represented by a dot on top of the variable, $u(\cdot)$ is the input to the linear system, $x(\cdot)$ is the system state, and the output of the system is $y(\cdot)$.

Next, the modeling of the hysteresis and structural vibrations is described, beginning with a description of the experimental setup.

A. Experimental Setup

The main components of the experimental system used in this study are a sectored piezoprobe that is used for scanning (lateral displacement) and an inductive sensor that measures this lateral displacement. The lateral motion of the piezoactuator is achieved by applying voltages across opposite electrodes of the sectored piezoactuator. The complete experimental system also includes amplifiers for the piezoactuator and the electronics needed to condition the sensor outputs. The input to the system $V_a(t)$ is the input command to the piezoactuator's preamplifier, and the output of the system $y(t)$ is the piezoactuator's lateral deflection, measured by an inductive sensor.

B. Modeling of Hysteresis

The hysteresis curve for our system was obtained by applying a triangular-shaped voltage to the piezoactuator at a low frequency (0.5 Hz). At low frequencies (relative to the first resonant frequency of the piezoactuator system), the structural vibrations have little effect on the output response and are neglected. The resulting input-output response is shown in Fig. 2a. Note that the hysteresis curves depend on the amplitude of applied voltage and are also rate dependent; these are ignored in the present work. However, even with the significantly simplified models, we show that an inversion-based approach can lead to substantial improvements in output tracking precision.

One method used to model the hysteresis is curvefitting of the observed hysteresis nonlinearity using polynomials.[13] These polynomial models can then be inverted to obtain the inverse-hysteresis model. In contrast, we directly model the inverse hysteresis using polynomials. The inverse of the hysteresis nonlinearity is obtained by swapping the axes of Fig. 2a and plotting the applied voltage $V_a(t)$ as a function of the normalized output of the hysteresis model

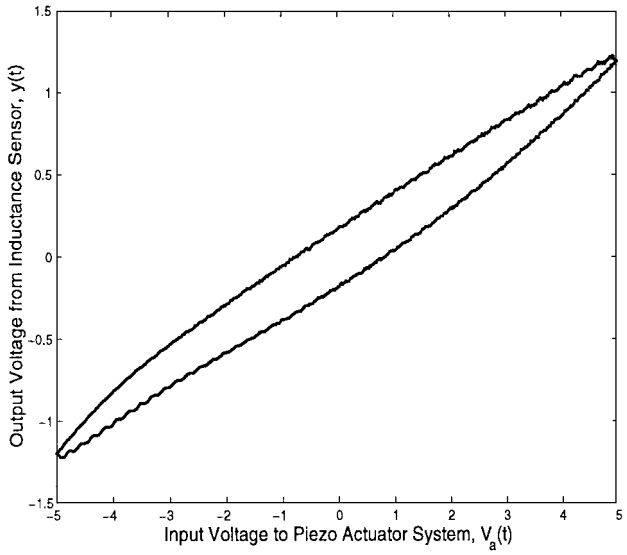

a) Hysteresis nonlinearity

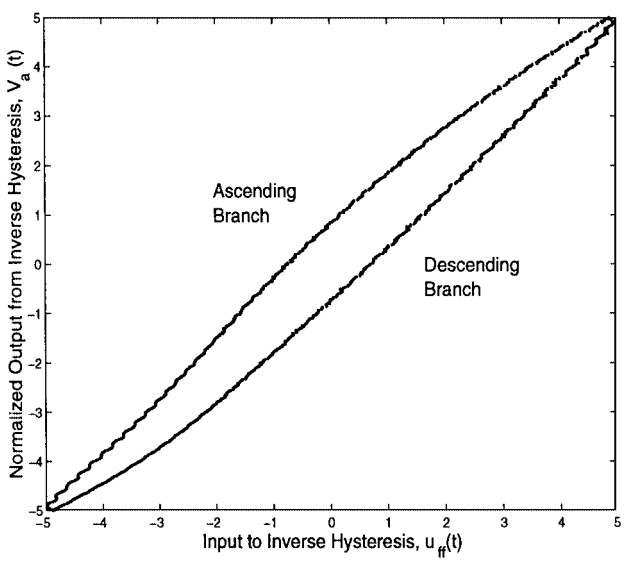

b) Inverse hysteresis nonlinearity

Fig. 2 Hysteresis nonlinearities of piezoactuator system.

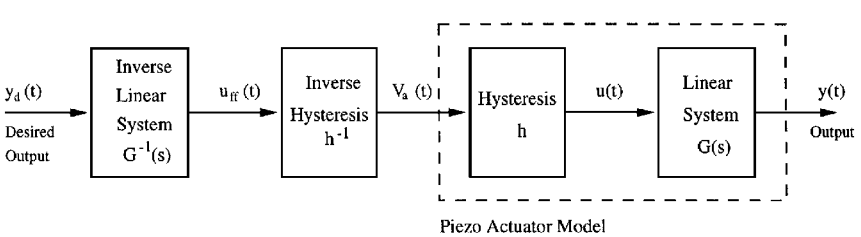

Fig. 1 Piezoactuator model with inverse.

as in Fig. 2b. Note that the dc gain factor (amplification between the input voltage and the output piezoactuator displacement for a constant input) is included in the modeling of the linear system $G(s)$.

This inverse-hysteresis curve (which has near point symmetry about the origin) is modeled as a third-order polynomial, with different polynomials for the ascending and descending curves (branches) as shown in Fig. 2b. These third-order polynomials are given by

$$V_a(t) = au_{ff}(t)^3 + bu_{ff}(t)^2 + cu_{ff}(t) + d \tag{3}$$

$$V_a(t) = au_{ff}(t)^3 - bu_{ff}(t)^2 + cu_{ff}(t) - d \tag{4}$$

where Eqs. (3) and (4) are the input voltages to the piezosystem for the ascending and descending branch, respectively, and $u_{ff}(t)$ represents the input to the inverse-hysteresis model (see Fig. 1).

The data were then fitted in a least-squares sense to give $a = -0.0042$, $b = -0.0303$, and $c = 1.089$. The d term in the preceding polynomials depends on when a change in direction of the voltage occurs, i.e., whether the voltage changes from increasing to decreasing or vice versa. If the direction change occurs at an input voltage $u_{ff}(t) = u_*$, between $\pm 5V$, then the constant d in Eqs. (3) and (4) is chosen as $d = d_u$ for an ascending branch, $d = d_l$ for a descending branch, where

$$d_u = V_* - au_*^3 - bu_*^2 - cu_* \tag{5}$$

$$d_l = V_* - au_*^3 + bu_*^2 - cu_* \tag{6}$$

Here V_* represents the output of the inverse hysteresis model at the time of the change of direction in $u_{ff}(t)$ (see Fig. 1).

As an example of hysteresis inversion, consider the voltage profile presented in Fig. 3a, which will be passed through the hysteresis inverse model. In region I, the voltage is increasing, and in region II, the voltage is decreasing. Thus d has to be found at the beginning of the motion and when the input direction changes between the two regions.

At $t = 0$, point A in the Fig. 3a, with zero initial conditions, i.e., $u_* = u_{ff}(0) = 0$, and zero applied input voltage $[V_* = V_a(0) = 0]$, d is found as

$$d = d_u = V_* - au_*^3 - bu_*^2 - cu_* \tag{7}$$

$$= 0 \tag{8}$$

The input voltage for region I (Fig. 3b) can then be determined using Eq. (3), with $d = 0$. At the next change in the input's direction (point B in Fig. 3a at $t = t_b$), the constant d is changed to

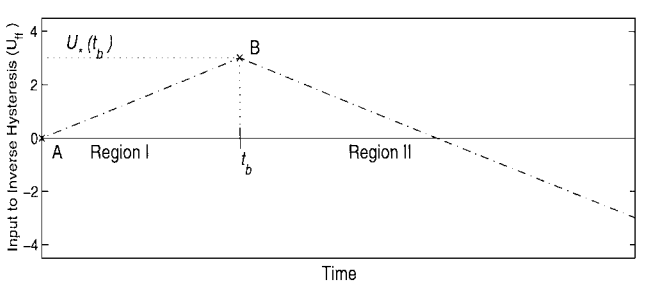

a) Input voltage

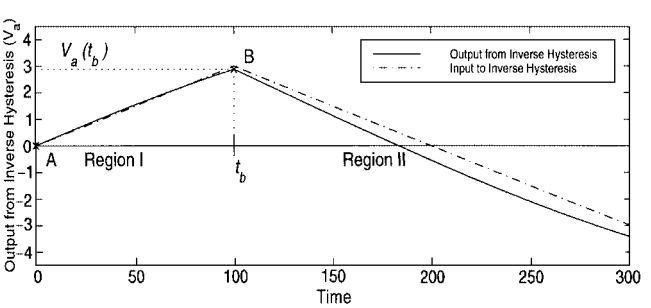

b) Output voltage

Fig. 3 Example of applying inverse-hysteresis model.

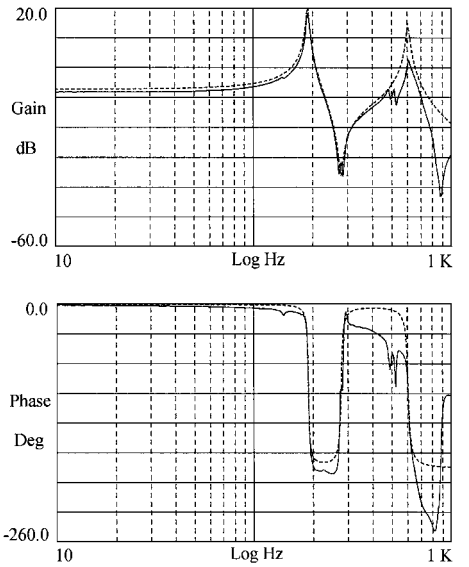

Fig. 4 Bode plots: comparison of model with experimental results. The fourth-order model captures the system behavior up to 185 Hz, the first vibrational frequency (——, experiment, and - - - -, model).

$$d = d_l = V_* - au_*^3 + bu_*^2 - cu_* \tag{9}$$

where $u_* = u_{ff}(t_b)$, and $V_* = V_a(t_b)$. The input voltage for region II can then be determined using Eqs. (4) and (9), with this new value of d. Thus for any desired input $u_{ff}(t)$, the hysteresis inverse can be determined by appropriately adjusting the constant d whenever the voltage direction changes.

C. Modeling of Piezodynamics

Once the input hysteresis is inverted, the remaining dynamics (structural vibrations) are modeled as a linear system; the linear model was found experimentally using a dynamic signal analyzer (HP3650A). The input command from the dynamic signal analyzer was 1) passed through the inverse-hysteresis model (implemented using a personal computer), 2) sent to the piezoactuator system, and 3) the resulting output was sent back to the dynamic signal analyzer. The Bode plot, found experimentally, is given in Fig. 4. The linear system was modeled as a fourth-order linear system, which includes the first two modes of vibration of the piezosystem. Higher-frequency modes can also be included, with added complexity, to improve the accuracy of the model. The present paper will show, however, that even by using a low-order model to find the linear system-inverse, it is possible to substantially improve the positioning speed of the piezoprobe system. Observe in Fig. 4 that 1) the fundamental vibrational frequency is at 185 Hz and that 2) the Bode plots (model and experiment) start to deviate significantly near this fundamental mode of vibration (185 Hz).

The resulting transfer function from the dynamic signal analyzer model can be written in state-space form as

$$\dot{x}(t) = Ax(t) + Bu(t) \tag{10}$$

$$y(t) = Cx(t) \tag{11}$$

with the state-space matrices defined as

$$A = \begin{bmatrix} 0 & 1 & 0 & 0 \\ 0 & 0 & 1 & 0 \\ 0 & 0 & 0 & 1 \\ -2.0659 \times 10^{13} & -5.6453 \times 10^{8} & -1.5967 \times 10^{7} & -164.28 \end{bmatrix}$$

$$B = [0 \quad 0 \quad 0 \quad 1]^T$$

$$C = [9.1521 \times 10^{12} \quad 1.6867 \times 10^{8} \quad 2.9992 \times 10^{6} \quad 0]$$

Note that the preceding state-space model is in the first companion form[26] and that there are four poles and two zeros. It is also easily verified that the poles of the system are all in the open-left-half complex plane, and hence the system is stable.

This completes the modeling of the piezoactuator dynamics. To summarize, the hysteresis and vibrations are modeled as cascaded subsystems; the inverse hysteresis is modeled using Eqs. (3) and (4), and the resulting linearized system is modeled using Eqs. (10) and (11).

III. Inversion-Based Output Tracking Scheme

Given a desired position trajectory $y_d(\cdot)$, the inversion problem is to find an input-voltage trajectory that achieves exact tracking of the desired output trajectory. This inversion is decoupled into two subproblems: 1) the inversion of the hysteresis input nonlinearity and, having done that, 2) the inversion of the linearized system. This approach is represented in Fig. 1.

The inverse-hysteresis model is determined using the polynomial approach described in Eqs. (3) and (4). The inverse for the linear model, $G(s)$, is described next.[10,11,24]

Given a desired position trajectory $y_d(\cdot)$, the problem is to find an input-voltage trajectory $u_{ff}(\cdot)$ and a state trajectory $x_{\text{ref}}(\cdot)$ such that the system equation (10) is satisfied and the position trajectory is achieved exactly, i.e.,

$$\dot{x}_{\text{ref}}(t) = Ax_{\text{ref}}(t) + Bu_{ff}(t) \tag{12}$$

$$y_d(t) = Cx_{\text{ref}}(t) \tag{13}$$

This is done by repeatedly differentiating (with respect to time) the output $y(t) = Cx(t)$ in Eq. (11) until an explicit relationship appears between the input and the output. The first time derivative of the output yields

$$\dot{y}(t) = C\dot{x}(t) \tag{14}$$

$$= C[Ax(t) + Bu(t)] \tag{15}$$

$$= CAx(t) \tag{16}$$

where it can be checked that $CB = 0$. Hence the dependence of the output's first time derivative with respect to the input is not explicit. The output is differentiated, again, to get

$$\ddot{y}(t) = CA\dot{x}(t) \tag{17}$$

$$= CA[Ax(t) + Bu(t)] \tag{18}$$

$$= CA^2x(t) + CABu(t) \tag{19}$$

with CAB nonzero for the present system; this is to be expected because the system (10) has a relative degree of 2 (Ref. 24), i.e., the number of poles minus the number of zeros is 2. Equation (19) is an explicit relationship between the output and the input. Thus the inverse input $u_{ff}(\cdot)$ that maintains exact tracking $y(\cdot) = y_d(\cdot)$ satisfies the relationship

$$\ddot{y}_d = CA^2x(t) + CABu_{ff}(t) \tag{20}$$

and yields the inverse input as

$$u_{ff}(t) = (CAB)^{-1}\left[\ddot{y}_d(t) - CA^2x(t)\right] \tag{21}$$

Note that the desired position trajectories have to be twice differentiable to apply the inversion for exact tracking as shown earlier. This is a necessary condition for exact tracking.[24]

The inverse of the linear system $u_{ff}(t)$ is then passed through the inverse-hysteresis model using Eqs. (3) and (4) to determine the voltage $V_a(t)$ that should be applied to the piezoactuator.

Feedback-based error correction, to correct for modeling errors or to increase convergence of nonzero initial error, can also be added to improve output tracking.[11]

IV. Results and Discussion

Five sets of experiments were performed: 1) applying $y_d(t)$ scaled up by the dc gain of the uncompensated system, i.e., without hysteresis or vibrational compensation; 2) using only hysteresis compensation without the vibration compensation; 3) using only hysteresis compensation without the vibration compensation but with Proportional Derivative (PD) feedback control; 4) using both vibration and hysteresis compensation; and 5) using both vibration and hysteresis compensation with PD feedback control.

The desired output trajectory (displacement trajectory) was chosen as a back and forth scanning with the piezoactuator and is shown in Fig. 5. Because a twice differentiable position trajectory is required, first an appropriate acceleration profile was chosen (see Fig. 5), and then the acceleration was integrated twice to determine the position trajectory. Output redesign[27] to optimally choose the desired scan path is also possible but was not done for this example. Also note that the desired position scan trajectory contains frequency components higher than the scanning frequency; this implies that it is important to model the higher-frequency dynamics of the piezosystem (even beyond the scanning frequency).

The results of the trajectory-tracking experiments are shown in Figs. 6–10. The applied voltages at 37 Hz, for each of the cases described earlier, are compared in Fig. 11. Note that without vibration or hysteresis compensation, the scan-path tracking is reasonable at low scan rates (18.5 Hz, i.e., one-tenth fundamental mode of vibration) (see Fig. 6); however, the effects of hysteresis and structural vibrations are clearly visible even at these low scanning frequencies. In Fig. 7, the low scan-rate (18.5 Hz) tracking performance is improved by using the hysteresis compensation (the rms error was decreased by 20%); however, vibration effects still cause tracking errors. In both Figs. 6 and 7, at the higher scan rate, the dynamic effects adversely affect the tracking performance of the piezoactuator. At 37-Hz scan rates (one-fifth the fundamental mode of vibration), errors due to the vibrations are substantial and the scan-path tracking is poor. In Fig. 8, the addition of PD feedback control improves the low scan rates (18.5 Hz) but fails to significantly suppress the vibrations of the higher scan rate (37 Hz). Thus, the fundamental vibrational frequency of the piezoactuator system limits the achievable scan rates. Increases in the fundamental vibrational frequency of the piezoactuator system and thereby increases in the tracking bandwidth can be achieved, for example, by shortening the piezoactuator. However, this tends to reduce the achieved positioning ranges. Therefore large range and high bandwidth are not achievable at the same time due to vibrational considerations.[12] In contrast, Fig. 9 shows that the addition of inversion-based feed

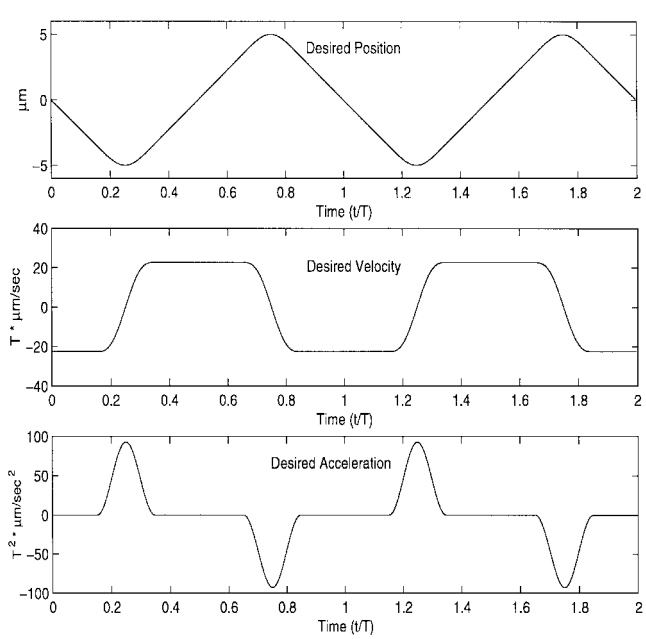

Fig. 5 Desired scan trajectories where T is the scan period. The desired position trajectory is twice differentiable.

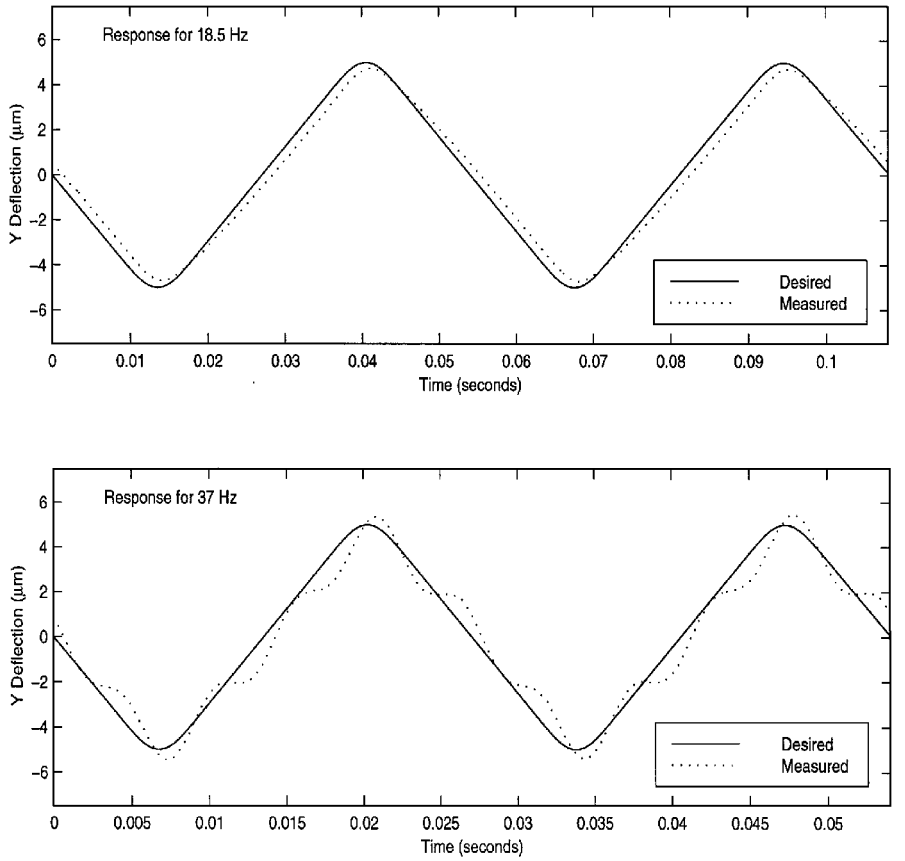

Fig. 6 Scan-path tracking without vibration and without hysteresis compensation. Although reasonable tracking is achieved for the 18.5-Hz scan rate, the vibrations result in a loss of tracking at the 37-Hz scan rate.

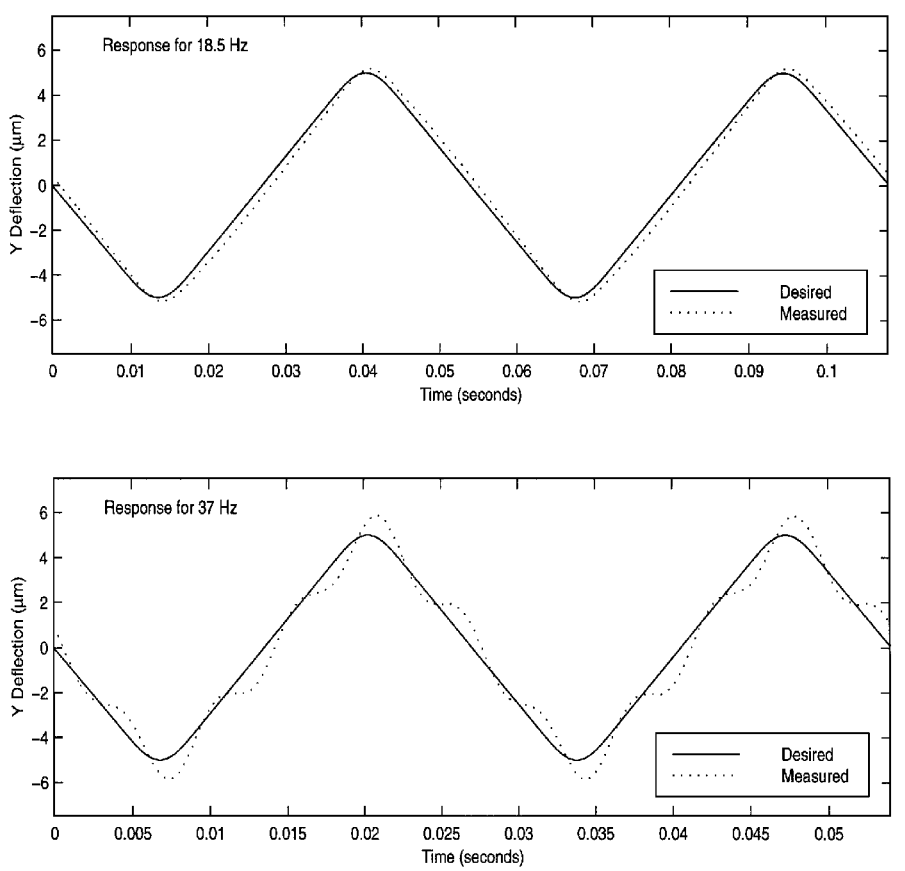

Fig. 7 Scan-path tracking with hysteresis compensation but without vibration compensation. Structural vibrations still cause loss of tracking for the 37-Hz scan rate.

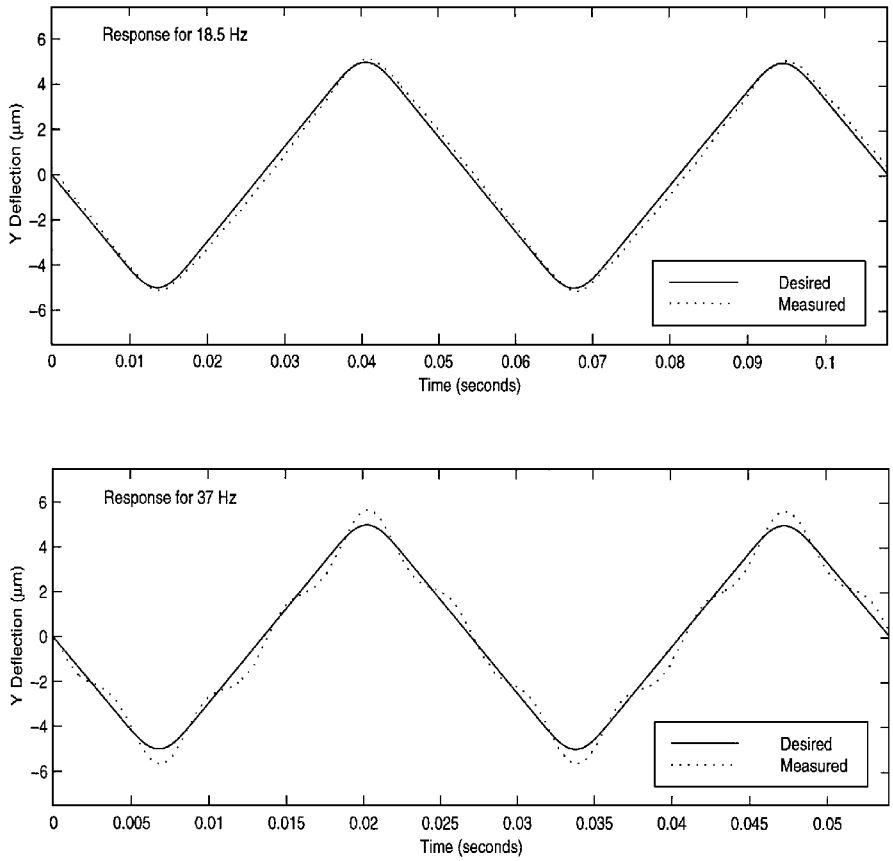

Fig. 8 Scan-path tracking with hysteresis compensation and PD feedback but without vibration compensation. The addition of feedback (compared with Fig. 7) improves tracking but not sufficiently at the 37-Hz scan rate.

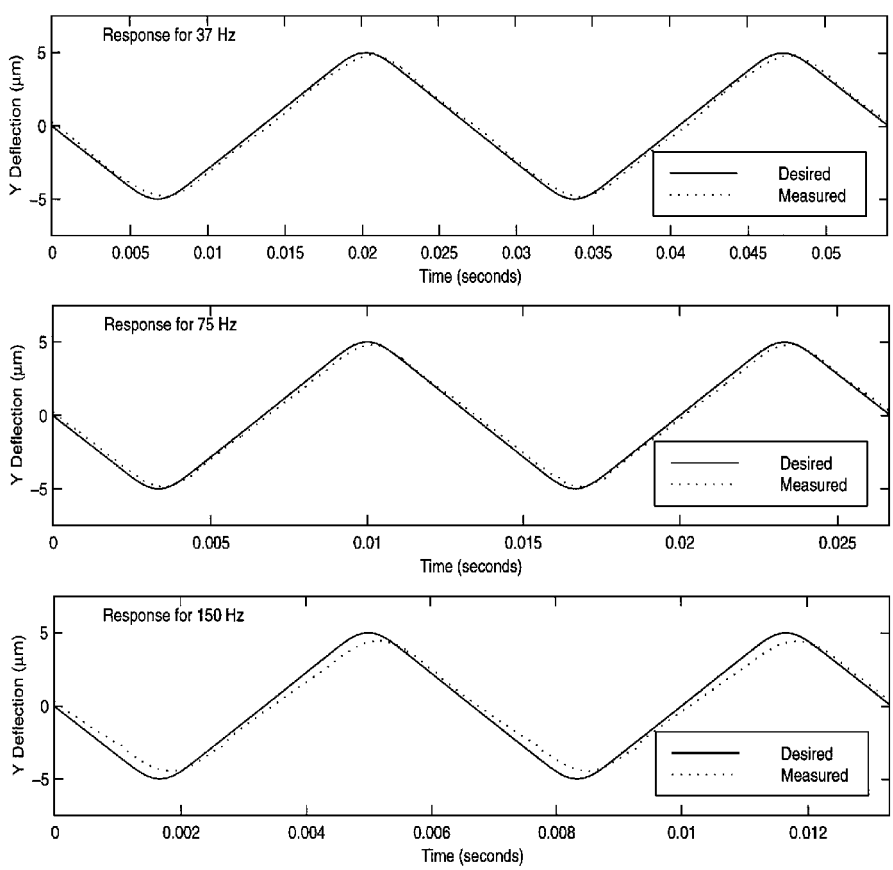

Fig. 9 Scan-path tracking with vibration and with hysteresis compensation but without feedback compensation. The addition of vibration compensation substantially improves tracking performance (compared with tracking for 37 Hz in Figs. 7 and 8).

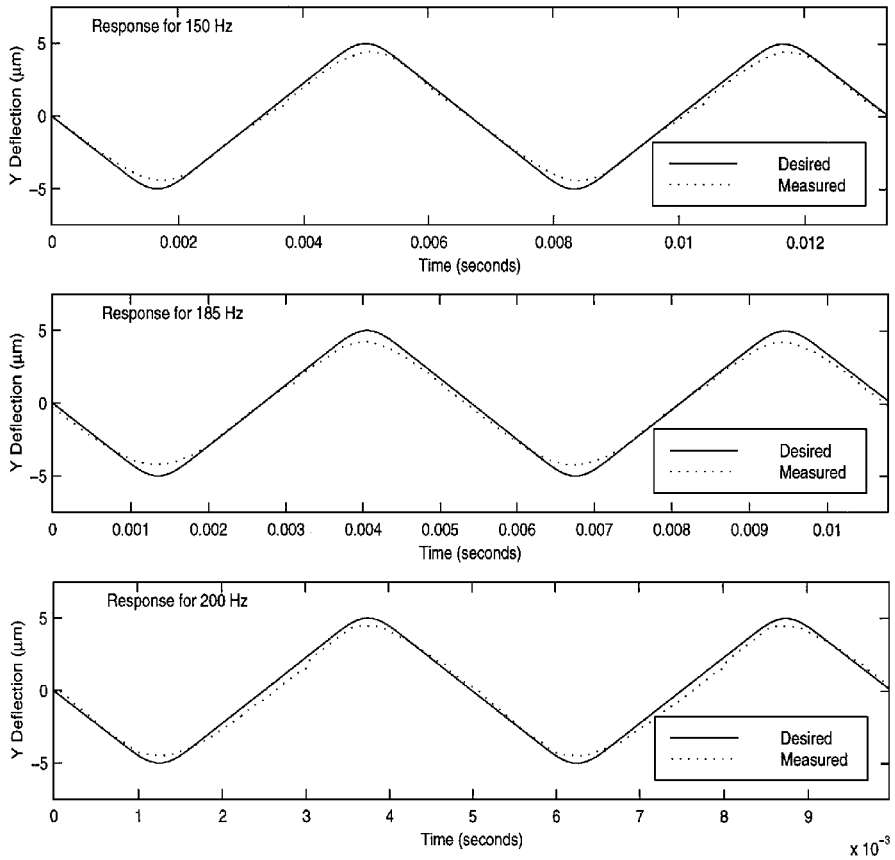

Fig. 10 Scan-path tracking with vibration and hysteresis compensation and PD feedback. With the addition of PD feedback, tracking is achieved at frequencies even beyond the fundamental vibrational frequency.

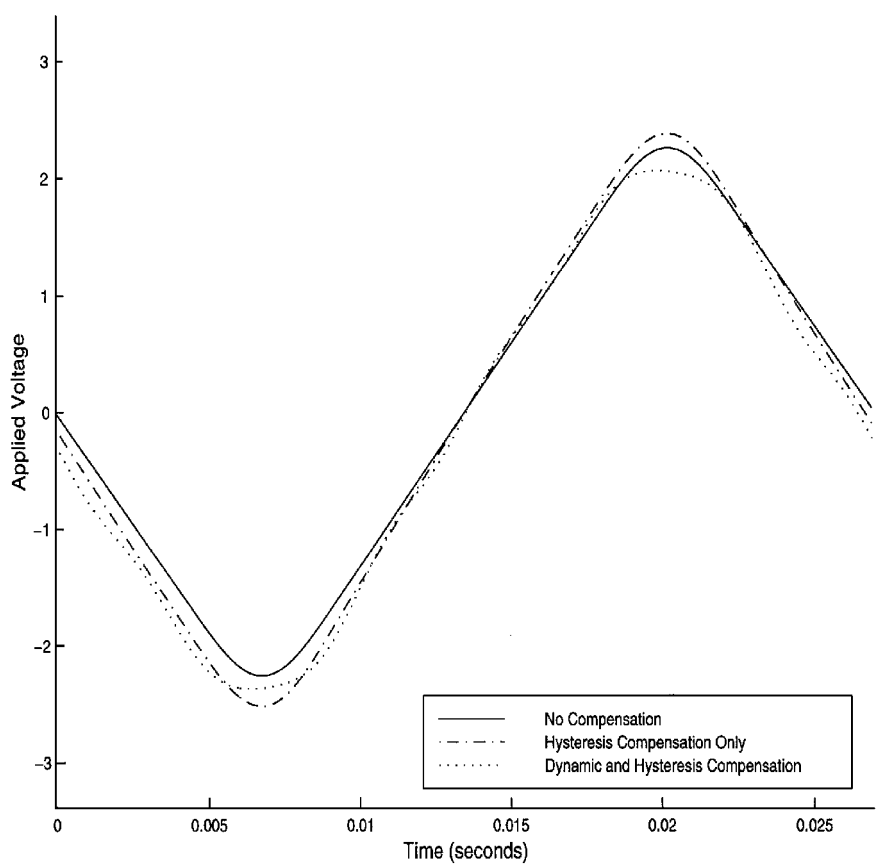

Fig. 11 Comparison of applied voltage to piezosystem for a 37-Hz scan rate. The magnitudes of the modified inputs are similar to the magnitude of the unmodified input but result in substantial performance improvements in tracking.

forward with hysteresis compensation substantially improves the tracking of the piezoprobe. In particular note that these significant improvements in positioning are achieved with applied voltages that have similar magnitudes (see Fig. 11). To illustrate the efficacy of the approach, we show the positioning results for a 75-Hz scan rate, at which tracking is not possible without vibration compensation (see Fig. 9). Even at 150 Hz, only minor deviations in scan-path tracking are observed, and path tracking is still comparable to that achieved by the other two techniques at much lower scan rates (for example, compare the 150-Hz scan rate in Fig. 9 with the 18.5-Hz scan rates in Figs. 6 and 7). With the addition of PD feedback control to the inversion-based approach (to correct for modeling errors), the performance is improved further. The precision of tracking at 150 Hz is improved, and tracking is achieved even at the resonant frequency of the piezosystem (see Fig. 10).

These improvements in scan-path tracking are achieved because both the hysteresis nonlinearities and the structural dynamics are included in the computation of the feed-forward input to the piezoprobe. Previous works[14,22] and our experimental results have verified that hysteresis compensation (used alone) improves the tracking performance of the piezoprobe at low frequencies (such as 1 Hz for our system), but at higher frequencies the errors due to the structural vibrations of the piezosystem become more dominant than the errors due to hysteresis effects. Thus, for a fixed scan rate the hysteresis compensation becomes important when larger scan ranges are needed. In contrast, if the scan range is kept fixed and the scan rates are increased, then the vibration compensation becomes more important. In conclusion, to achieve both, high precision and high speed, combined hysteresis and vibration compensation is needed.

The experimental results show that it is possible to achieve precision scanning of piezoprobes at their fundamental vibrational frequency (i.e., the bandwidth of the piezoprobe has effectively been increased from one-tenth the fundamental frequency of vibration to the fundamental frequency). If shorter piezos with 1–5 kHz fundamental vibrational frequencies are used—as is typical in scanning tunneling microscopy[12,28]—then scan rates can be increased further.

Note that, at present, the only limitation to increasing the scan rate and precision is the modeling error. It is expected that, by using more detailed models of both the hysteresis nonlinearities and higher-order dynamics of the piezoprobe, the scan rates can be increased further with increased precision. These are currently under study.

V. Conclusion

The inversion-based approach is used to successfully compensate for two of the fundamental limitations when using piezoactuators for precision positioning: nonlinear hysteresis and structural vibrations. The hysteresis was modeled as an input nonlinearity, and the resulting linearized system (vibrational dynamics) was inverted to find input voltages that achieve exact tracking of a desired position trajectory. Experimental results show that significant improvements in precision tracking are possible with an order of magnitude increase in tracking bandwidth; a bandwidth approaching the first fundamental vibrational frequency of the piezoactuator system was experimentally demonstrated.

Acknowledgment

This work was supported by the National Science Foundation under Grant DMI-9612300.

References

[1]Crawley, E. F., "Intelligent Structures for Aerospace: A Technology Overview and Assessment," *AIAA Journal*, Vol. 32, No. 8, 1994, pp. 1689–1699.

[2]Barrett, R., "Active Plate and Missile Wing Development Using Directionally Attached Piezoelectric Elements," *AIAA Journal*, Vol. 32, No. 3, 1994, pp. 601–609.

[3]Foecke, T., King, R. M., Dale, A. F., and Gerberich, W. W., "Imaging of Cracks in Semiconductors Using Scanning Tunneling Microscopy," *Journal of Vacuum Science and Technology*, Vol. B9, No. 2, 1991, pp. 673–676.

[4]De Lozanne, A. L., Smith, W. F., and Ehrichs, E. E., "Direct Writing with a Combined STM/SEM System," *Proceedings of NATO Advanced Research Workshop on Nanolithography: A Borderland between STM, EB, IB, and X-ray Lithographies*, Vol. 264, NATO ASI Series E: Applied Science, Frascati, Roma, Italy, 1993, pp. 159–174.

[5]Moriyama, S., Uchida, F., and Seya, E., "Development of a Precision Diamond Turning Machine for Fabrication of Asymmetric Aspheric Mirrors," *Optical Engineering*, Vol. 27, No. 11, 1998, pp. 1008–1012.

[6]Hirschorn, R. M., "Invertibility of Multivariable Nonlinear Control Systems," *IEEE Transactions on Automatic Control*, Vol. AC-24, No. 6, 1979, pp. 855–865.

[7]Isidori, A., and Byrnes, C. I., "Output Regulation of Nonlinear Systems," *IEEE Transactions on Automatic Control*, Vol. 35, No. 2, 1990, pp. 131–140.

[8]Devasia, S., Chen, D., and Paden, B., "Nonlinear Inversion-Based Output Tracking," *IEEE Transactions on Automatic Control*, Vol. 41, No. 7, 1996, pp. 930–942.

[9]Devasia, S., and Bayo, E., "Redundant Actuators to Achieve Minimal Vibration Trajectory Tracking of Flexible Multibodies: Theory and Application," *Nonlinear Dynamics*, Vol. 6, No. 4, 1994, pp. 419–431.

[10]Silverman, L. M., "Inversion of Multivariable Linear Systems," *IEEE Transactions on Automatic Control*, Vol. AC-14, No. 3, 1969, pp. 270–276.

[11]Croft, D., McAllister, D., and Devasia, S., "High-Speed Scanning of Piezo-Probes for Nano-fabrication," *ASME Journal of Manufacturing Science and Engineering* (to be published).

[12]Pohl, D. W., "Some Design Criteria in Scanning Tunneling Microscopy," *IBM Journal of Research and Development*, Vol. 30, No. 4, 1986, pp. 417–427.

[13]Holman, A. E., Scholte, P. M. L. O., Heerens, W. C., and Tuinstra, F., "Analysis of Piezo Actuators in Translation Constructions," *Review of Scientific Instruments*, Vol. 66, No. 5, 1995, pp. 3208–3215.

[14]Ge, P., and Jouaneh, M., "Tracking Control of a Piezoceramic Actuator," *IEEE Transactions on Control Systems Technology*, Vol. 4, No. 3, 1996, pp. 209–216.

[15]Koops, R., and Sawatzky, G. A., "New Scanning Device for Scanning Tunneling Microscope Applications," *Review of Scientific Instruments*, Vol. 63, No. 8, 1992, pp. 4008, 4009.

[16]Barrett, R. C., and Quate, C. F., "Optical Scan-Correction System Applied to Atomic Force Microscopy," *Review of Scientific Instruments*, Vol. 62, No. 6, 1991, pp. 1393–1399.

[17]Main, J. A., and Garcia, E., "Piezoelectric Stack Actuators and Control System Design: Strategies and Pitfalls," *Journal of Guidance, Control, and Dynamics*, Vol. 20, No. 3, 1997, pp. 479–485.

[18]Tamer, N., and Dahleh, M., "Feedback Control of Piezoelectric Tube Scanners," *Proceedings of the 33rd Conference on Decision and Control*, IEEE Control Systems Society, Lake Buena Vista, FL, 1994, pp. 1826–1831.

[19]Newcomb, C. V., and Flinn, I., "Improving the Linearity of Piezoelectric Ceramic Actuators," *Electronics Letters*, Vol. 18, No. 11, 1982, pp. 442–444.

[20]Kaizuka, H., "Application of Capacitor Insertion Method to Scanning Tunneling Microscopes," *Review of Scientific Instruments*, Vol. 60, No. 10, 1989, pp. 3119–3122.

[21]Akila, J., and Wadhwa, S. S., "Correction for Nonlinear Behavior of Piezoelectric Tube Scanners Used in Scanning Tunneling and Atomic Force Microscopy," *Review of Scientific Instruments*, Vol. 66, No. 3, 1995, pp. 2517–2519.

[22]Schafer, J., and Janocha, H., "Compensation of Hysteresis in Solid-State Actuators," *Sensors and Actuators*, Vol. A49, June 1995, pp. 97–102.

[23]Lapshin, R. V., "Analytical Model for the Approximation of Hysteresis Loop and Its Application to the Scanning Tunneling Microscope," *Review of Scientific Instruments*, Vol. 66, No. 9, 1995, pp. 4718–4730.

[24]Isidori, A., *Nonlinear Control Systems*, 3rd ed., Springer–Verlag, New York, 1995, pp. 137–147, 162–172.

[25]Goldfarb, M., and Celanovic, N., "Modeling Piezoelectric Stack Actuators for Control of Micromanipulation," *IEEE Control Systems*, Vol. 17, No. 3, 1997, pp. 69–79.

[26]Friedland, B., *Control System Design*, McGraw–Hill, New York, 1986, pp. 88–97.

[27]Devasia, S., "Optimal Output Trajectory Redesign for Invertible Systems," *Journal of Guidance, Control, and Dynamics*, Vol. 19, No. 5, 1996, pp. 1189–1191.

[28]Park, S., and Quate, C. F., "Theories of the Feedback and Vibration Isolation Systems for the Scanning Tunneling Microscope," *Review of Scientific Instruments*, Vol. 58, No. 11, 1987, pp. 2004–2009.